N90-20548

VERY ACCURATE UPWARD CONTINUATION TO LOW HEIGHTS IN A TEST OF NON-NEWTONIAN THEORY

Anestis J. Romaides and Christopher Jekeli
Air Force Geophysics Laboratory, Hanscom AFB, MA, 01731

Abstract

Recently, gravity measurements were made on a tall, very stable televsion transmitting tower in order to detect a non-Newtonian gravitational force. This experiment required the upward continuation of gravity from the Earth's surface to points as high as only 600 m above ground. The upward continuation was based on a set of gravity anomalies in the vicinity of the tower whose data distribution exhibits essential circular symmetry and appropriate radial attenuation. Two methods were applied to perform the upward continuation - least-squares solution of a local harmonic expansion and least-squares collocation. Both methods yield comparable results, and have estimated accuracies on the order of 50 μGal or better (1 μGal = 10^{-8} m/s^2). This order of accuracy is commensurate with the tower gravity measurements (which have an estimated accuracy of 20 μGal), and enabled a definitive detection of non-Newtonian gravity. As expected, such precise upward continuations require very dense data near the tower. Less expected was the requirement of data (though sparse) up to 220 km away from the tower (in the case that only an ellipsoidal reference gravity is applied).

1. INTRODUCTION

The upward continuation may be summarized as follows. A set of surface gravity anomalies, circularly symmetric about the tower, serves as the set of boundary values. The upward continuation is based on Newtonian theory either through a local harmonic series expansion of the potential or through the use of least-squares collocation. At altitude, the (upward continued) GRS67 normal gravity and attraction of the atmospheric layer are added to the upward continued gravity anomaly. The result is the total gravity as would be observed in a strictly Newtonian world. A comparison with the gravity directly observed using a gravimeter offers a test of the underlying theory.

2. THE MATHEMATICS OF UPWARD CONTINUATION

If V denotes the earth's gravitational potential, then under Newtonian potential theory, V satisfies Laplace's differential equation in free space:

$$\nabla^2 V = 0. \tag{1}$$

One solution to Laplace's equation (1) is a Fourier-Bessel series expansion in cylindrical coordinates, which is appropriate for a local representation of the potential. Thus, since in the planar approximation the gravity anomaly is also a harmonic function (it satisfies Laplace's equation in free space), it may be expressed as the following series (Morse and Feshbach, 1953, pp. 1259-1262):

$$\Delta g(\rho,\theta,z) = \sum_{n=-\infty}^{\infty} \int_0^{\infty} C_n(k)\, J_n(k\rho)\, e^{-kz-in\theta} dk, \tag{2}$$

where ρ is radial distance in the horizontal plane, θ is azimuth, and z is altitude. J_n is the Bessel function of the first kind and n-th order, k is

the wavenumber in the radial direction, and the C_n are coefficient functions to be determined from gravity anomaly data. Since the final evaluation of (2), once the C_n are known, is along the vertical, ρ=0, this problem is simplified by defining an azimuthal average:

$$\overline{\Delta g}(\rho,z) = \frac{1}{2\pi}\int_0^{2\pi}\Delta g(\rho,\theta,z)\,d\theta = \int_0^{\infty}C_0(k)\,J_0(k\rho)\,e^{-kz}\,dk\ . \qquad (3)$$

This average coincides with the unaveraged Δg along the vertical:

$$\overline{\Delta g}(0,z) = \Delta g(0,\theta,z) = \int_0^{\infty}C_0(k)\,e^{-kz}\,dk\ . \qquad (4)$$

The second equality in (4) follows by noting that at ρ=0 all J_n's in (2) are zero except J_0 which is one. It remains, therefore, to determine only the function C_0 from azimuthally averaged gravity anomaly data. One can determine at best a finite set of values of C_0 from a discrete and finite data set. The integral (3), therefore, is truncated to some finite limit and discretized. The truncation is optimized if the discretization is in the form of a Fourier-Bessel expansion. After making the appropriate substitutions in replacing the integral (3) with the discrete summation (see Romaides et al., 1988), the least-squares solution is obtained by the following:

$$\sum_{p=1}^{P}\left[f_p - \sum_{m=1}^{M}A_m\,J_0(\xi_p\kappa_m)\,\exp\left(\frac{-\kappa_m}{R}(z_p - z_0)\right)\right]^2 \longrightarrow \min., \qquad (5)$$

where P is the number of points, M is the number of zeros, κ_m are the zeros of J_0, $f_p = \Delta g(\xi_p R,\theta_p,z_p) - \overline{\Delta g}(R,z)$, $\xi_p = \rho/R$, R is the maximum radius of surface data, z_0, z_p are the elevations of the tower base and surface points, and A_m are the solution coefficients.

The Fourier-Bessel upward continuation then proceeds in three steps. An initial expansion is done using 23 zeros and approximately 1800 anomalies out to 220 km from the tower. This expansion allows the resolution of half-wavelengths down to about 5 km. A second expansion is then done on only the residuals inside of 5 km (from the tower) allowing resolution of half-wavelengths down to about 100 m. And finally a third expansion is done on the second set of residuals inside of 50 m from the tower resolving half-wavelengths down to about 20 m. Table 1 shows the results of the three steps, and Figure 1 is a contour map of the final set of residuals.

The other upward continuation method used is least-squares collocation which is an optimal estimation method based on the validity of Laplace's equation. All important in LSC estimation is a good representation of the covariance function of Earth's anomalous gravity field. The covariance model employed for the tower experiment consists of the actual degree variances of the Rapp-1981 field up to degree 30 (1300 km wavelengths) plus a sum of 9 reciprocal distance models (see Jekeli, 1984) each covering a specific band of wavelengths shorter than 1300 km. These models are fitted to a sequence of periodograms based on the gravity anomaly data. Figure 2 shows these periodograms along with the power spectral density of the final model. The model psd at wavelengths shorter than 300 m represents a rough

extrapolation. Figure 3 shows a plot of the collocation weights that are applied to ~270 data points; note the increase in the last two sets of weights which could be an artifact of oversampling.

3. CONCLUSION

The upward continuation of the surface gravity anomalies was done using two independent computation methods. The two methods are in excellent agreement (see Table 2) with both results clearly showing a departure from the inverse-square law. The conclusion is that there is a dominantly attractive non-Newtonian component to gravity. Previous experiments had indicated a repulsive component to gravity. This inconsistency can be overcome by postulating the existence of two additional forces, one attractive and one repulsive. Our data do not contain adequate resolution to distinguish between the one force (scalar) and two force (scalar-vector) models but are consistent with both. Figures 4 and 5 show plots of the two models along with our data. The error bars used are those of the first method.

REFERENCES

Jekeli, C., "Analysis of airborne gravity gradiometer survey accuracy," Manuscripta Geodaetica, vol.9, no.4, pp.323-379, 1984.

Morse, P.M., and H. Feshbach, Methods of Theoretical Physics, McGraw-Hill Book Company, Inc., New York, 1953.

Romaides, A.J., C. Jekeli, A.R. Lazarewicz, D.H. Eckhardt, and R.W. Sands, "A Detection of Non-Newtonian Gravity," Journal Of Geophysical Research, accepted for publication, 1988.

Table 1.

FOURIER-BESSEL UPWARD CONTINUATION

ELEVATION	STEP 1	STEP 2	STEP 3
0.69	.422	.266	.009
7.58	.256	.116	.002
9.38	.233	.098	.008
23.07	.094	-.013	-.013
45.93	-.054	-.121	-.098
68.76	-.159	-.196	-.176
93.92	-.187	-.199	-.184
192.17	-.341	-.306	-.301
283.58	-.455	-.414	-.412
379.54	-.534	-.499	-.498
473.24	-.567	-.541	-.540
562.27	-.566	-.548	-.547

Table 2.

OBSERVED MINUS PREDICTED (μGal)

ELEVATION	METH 1	ERROR	METH 2	ERROR
0.69	9	59	35	9
7.58	2	59	-2	13
9.38	8	59	0	16
23.07	-13	58	-27	36
45.93	-98	57	-100	61
68.76	-176	56	-171	80
93.92	-184	54	-179	95
192.17	-301	48	-304	117
283.58	-412	44	-413	120
379.54	-498	38	-493	120
473.24	-540	37	-528	121
562.27	-547	36	-526	121

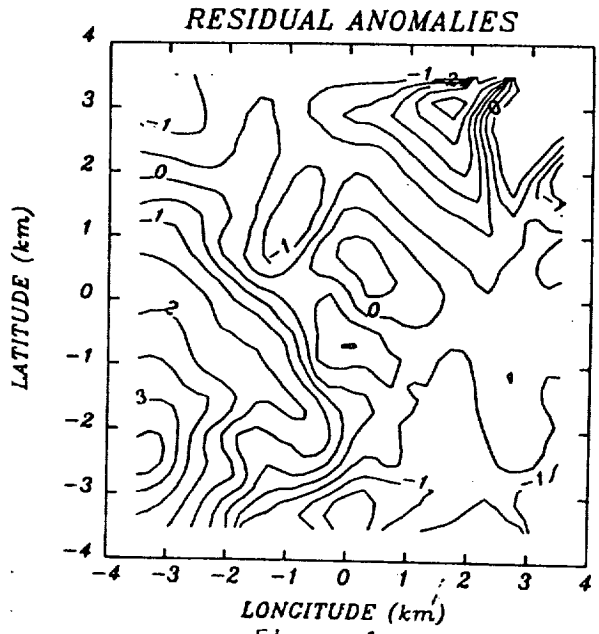

Figure 1.

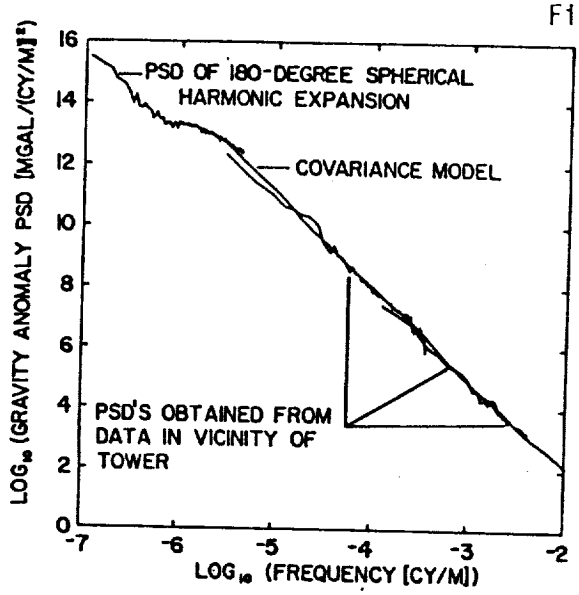

Figure 2.

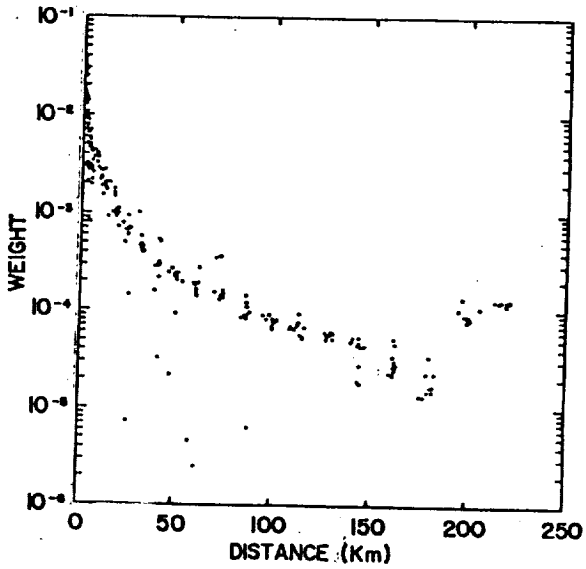

Figure 3.

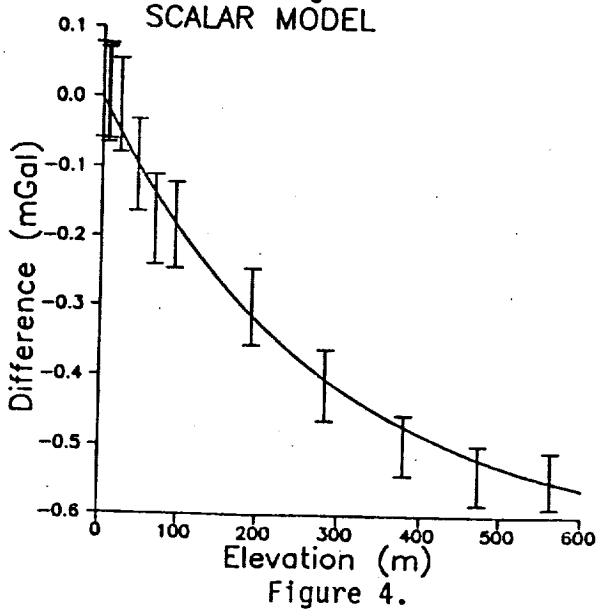

Figure 4.

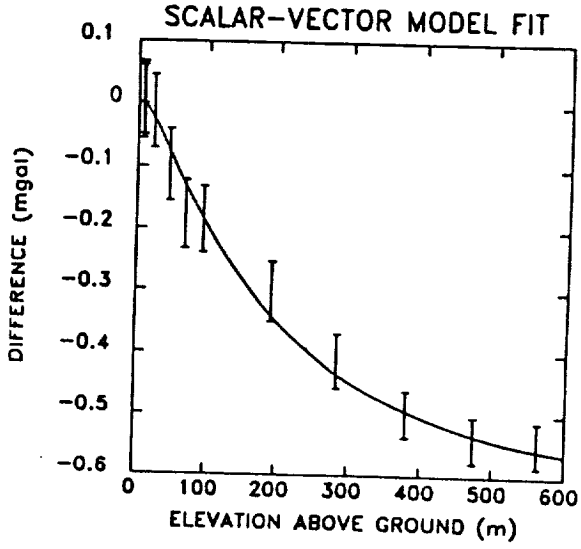

Figure 5.